

# A single intravenous injection of oncolytic picornavirus SVV-001 eliminates medulloblastomas in primary tumor-based orthotopic xenograft mouse models

Litian Yu, Patricia A. Baxter, Xiumei Zhao, Zhigang Liu, Lalita Wadhwa, Yujing Zhang, Jack MF Su, Xiaojie Tan, Jianhua Yang, Adekunle Adesina, Lazlo Perlaky, Mary Hurwitz, Neeraja Idamakanti, Seshidhar Reddy Police, Paul L. Hallenbeck, Susan M. Blaney, Murali Chintagumpala, Richard L. Hurwitz, and Xiao-Nan Li

Laboratory of Molecular Neuro-oncology (L.Y., X.Z., Z.L., Y.Z., X.-N.L.), Texas Children's Cancer Center (L.Y., P.A.B., X.Z., Z.L., L.W., Y.Z., J.M.F.S., X.T., J.Y., L.P., M.H., S.M.B., M.C., R.L.H., X.-N.L.), Center for Cell and Gene Therapy (L.W., M.H., R.L.H.), Department of Pathology (J.M.F.S., A.A.), Department of Pediatrics (A.A., M.H., S.M.B., M.C., R.L.H., X.-N.L.), Department of Ophthalmology (M.H., R.L.H.), Department of Molecular and Cellular Biology (M.H., R.L.H.), Texas Children's Hospital, Baylor College of Medicine, Houston, Texas; Neotropix, Inc., Malvern, Pennsylvania (N.I., S.R.P., P.L.H.)

Difficulties of drug delivery across the blood–brain barrier (BBB) and failure to eliminate cancer stem cells (CSCs) are believed to be the major causes of tumor recurrences in children with medulloblastoma (MB). Seneca Valley virus-001 (SVV-001) is a naturally occurring oncolytic picornavirus that can be systemically administered. Here, we report its antitumor activities against MB cells in a panel of 10 primary tumor-based orthotopic xenograft mouse models. We found that SVV-001 killed the primary cultured xenograft cells, infected and replicated in tumor cells expressing CSC surface marker CD133, and eliminated tumor cells capable of forming neurospheres in vitro in 5 of the 10 xenograft models. We confirmed that SVV-001 could pass through BBB in vivo. A single i.v. injection of SVV-001 in 2 anaplastic MB models led to widespread infection of the preformed intracerebellar (ICb) xenografts, resulting in significant increase in survival (2.2–5.9-fold) in both models and complete elimination of ICb xenografts in 8 of the 10 long-term survivors. Mechanistically, we showed that the intracellular replication of SVV-001 is mediated through a subverted

autophagy that is different from the bona fide autophagic process induced by rapamycin. Our data suggest that SVV-001 is well suited for MB treatment. This work expands the current views in the oncolytic therapy field regarding the utility of oncolytic viruses in simultaneous targeting of stem and nonstem tumor cells.

**Keywords:** cancer stem cells, medulloblastoma, oncolytic virus, orthotopic xenograft.

**M**edulloblastoma (MB) is the most common malignant brain tumor in children. Despite multimodal therapies, approximately 30% of children with MB experience tumor recurrence, and 5-year survival remains less than 10% in these patients with recurrent MB. No promising new treatment is on the horizon.<sup>1</sup> Invasive/metastatic growth (particularly in the anaplastic subtype of MB) and the difficulties of effective drug delivery through the blood–brain barrier (BBB) have long been the challenges of MB therapy. Recently, a new hypothesis has been proposed to explain the treatment failure and tumor recurrence in human cancers. According to this hypothesis, a small population of tumor cells, often designated as “tumor-initiating cells” or “cancer stem cells (CSCs),” are inherently resistant to existing therapies and possess exclusive self-renewal capacity to reinitiate tumor growth after treatment.<sup>2–7</sup> Indeed, enhanced resistance to

Received April 9, 2010; accepted August 20, 2010.

**Corresponding Author:** Xiao-Nan Li, MD, PhD, Texas Children's Cancer Center, Texas Children's Hospital, Baylor College of Medicine, 6621 Fannin St, MC 3-3320, Houston, TX 77030 (xiaonan@bcm.edu).

chemo- and radiotherapy has been demonstrated in human glioma CSCs and breast CSCs.<sup>8–11</sup> Elimination of CSCs is therefore necessary for the cure of human cancers.<sup>12,13</sup> However, direct targeting of stem cell–related signaling pathways may have the risk of harming normal stem cells, because many critical biological features of CSCs, including self-renewal, quiescence, and high levels of drug efflux proteins, are shared with normal stem cells.<sup>14,15</sup> Furthermore, CSCs constitute only a minor population of tumor cells. To maximize therapeutic efficacy, it is highly desired for new therapeutic strategies to eliminate both CSCs and nonstem tumor cells.

The use of oncolytic viruses presents an attractive approach for treating human cancers, including targeting CSCs.<sup>16–20</sup> Many oncolytic viruses possess cell-specific tropism that enables them to selectively attack cancer cells, including MBs.<sup>19,21</sup> They enter cells through infection and can target both proliferative and quiescent cells. They may therefore be able to evade the defense mechanisms of CSCs.<sup>12,21,22</sup> One additional advantage of the replication-competent oncolytic virus is that viral replication leads to oncolytic death of the cells, releasing thousands of virions that can infect and kill additional tumor cells.<sup>23</sup> Several oncolytic viruses have displayed cell-killing activities against human CSCs,<sup>20</sup> including the effective killing of glioblastoma CSCs and breast cancer–initiating CD44<sup>+</sup>CD24<sup>-/low</sup> cells with oncolytic adenoviruses and herpes simplex virus,<sup>12,24,25</sup> and the targeting of breast CSCs with oncolytic reovirus.<sup>23</sup> Many of the viruses tested, however, often require intratumoral injections, which may have suboptimal tumor distribution. Efforts are thus being made to develop oncolytic virus that can be systemically administered, such as oncolytic poxviruses and including vaccinia virus.<sup>26,27</sup>

The Seneca Valley virus-001 (SVV-001) is a native single-strand RNA virus that belongs to the family Picornaviridae.<sup>28–31</sup> It replicates only in the cytoplasm and does not integrate into the host genome. SVV-001 is not a human pathogen and has not been associated with diseases in mice and rats.<sup>29</sup> Furthermore, SVV-001 can be administered systemically, as the virus is not inhibited by any component of human blood, and pre-existing neutralizing antibodies against SVV-001 are rare in humans. It has displayed antitumor activities in tumors with neuroendocrine properties and killed metastatic retinoblastoma cells.<sup>29,32</sup> Its effects on CSCs and its mechanism of intracellular replication, however, remain elusive.

The current study was therefore set to determine if SVV-001 can infect and kill MB cells, including the differentiated tumor cells, the cells expressing known CSC marker CD133, and the cells possessing the self-renewal capabilities *in vitro*; and if *i.v.* injected SVV-001 can pass through the BBB to eliminate the preformed orthotopic xenograft tumors to significantly prolong animal survival times. Since the intracellular replication of SVV-001 plays a role in oncolytic cell lysis and contributes to the enhanced or “amplified” cell killing by infecting additional tumor cells, we examined whether such

intracellular replication is mediated by the activation of autophagy. Recognizing that the traditional cell lines may not faithfully replicate the biology of the originating tumor and well preserve the tumor stem cells,<sup>33,34</sup> we utilized 10 primary tumor-based orthotopic xenograft mouse models of MB as our source of CSCs. These models were established through direct injection of fresh surgical specimens into the cerebellum of RAG2/severe combined immunodeficiency (SCID) mice and are shown to have replicated the biology of the original patient tumors and preserved CD133<sup>+</sup> CSC pools.<sup>35</sup>

## Materials and Methods

### *The Virus*

SVV-001 ( $1 \times 10^{14}$  viral particle [vp]/mL) and the genetically engineered SVV-green fluorescent protein (GFP;  $1 \times 10^{12}$  vp/mL) were obtained from Neotropix.<sup>28,29,31</sup> SVV-GFP has identical tropism and infectivity as the parent SVV-001 but with reduced cell lysis activities. The median tissue culture infectious dose (TCID<sub>50</sub>) of SVV-001, the amount of SVV-001 that will produce pathological changes in 50% of cell cultures on the permissive cell line (per.c6), was  $2.12 \times 10^{12}$ /mL. For *in vitro* treatment, SVV-001 and SVV-GFP were diluted into serum-based Dulbecco’s modified Eagle’s medium for primary cultured cells and serum-free CSC growth medium containing epidermal growth factor (EGF) and basic fibroblast growth factor (bFGF) for CD133<sup>+</sup> cells and neurospheres. For *in vivo* treatment, SVV-001 was diluted with phosphate buffered saline and administered through a single tail vein injection.

### *Primary Tumor-Based Orthotopic Xenograft Mouse Models*

The Rag2 SCID mice, aged 5–7 weeks, were bred and housed in a specific pathogen-free animal facility at Texas Children’s Hospital in Houston. All the experiments were conducted using an Institutional Animal Care and Use Committee–approved protocol. Ten transplantable orthotopic xenograft mouse models of MB established by direct injection of fresh surgical specimens into mouse cerebella were included (Table 1). Eight of them have been reported previously.<sup>35</sup> These models are shown to have replicated the histopathological, genetic, and invasive/metastatic features of patient tumors and preserved the CD133<sup>+</sup> MB stem cell pool.

### *Cell Viability and Cytotoxicity Assay*

Primary cultured xenograft cells were seeded in 96-well plates in quadruplicate with or without SVV-001 at a multiplicity of infection (MOI) of 0.3–66. Cell viability was checked with Cell-Counting Kit-8 (CCK8; Dojindo Molecular Technologies), a “mix-and-measure”

**Table 1.** List of the primary tumor-based orthotopic xenograft mouse models of MB

Tumor ID	Age	Sex	Diagnosis (subtype)	Permissive to SVV001	Reference
ICb-1078MB	11 y 9 mo	Male	MB (anaplastic)	Yes	(new)
ICb-1299MB	2 y 9 mo	Female	MB (anaplastic)	Yes	35
ICb-984MB	7 y 10 mo	Female	MB (anaplastic)	Yes	35
ICb-1572MB	14 y 9 mo	Male	MB (anaplastic large cell)	Yes	35
ICb-1494MB	5 y 2 mo	Female	MB (anaplastic)	No	35
ICb-1595MB	15 mo	Male	MB (anaplastic)	No	(new)
ICb-1192MB	12 y 5 mo	Male	MB (classic)	No	35
ICb-1487MB	6 y 11 mo	Male	MB (classic)	Yes	(new)
ICb-1197MB	5 y	Male	MB (nodular)	No	35
ICb-1338MB	6 mo	Male	MB (nodular)	No	35

cell-counting assay, as we described previously.<sup>36</sup> To visualize viable tumor cells, we added 3-(4,5-dimethylthiazol-2-yl)-2,5-diphenyltetrazolium bromide (MTT) to the culture medium 3 hours before microscopy and photography.

#### Fluorescence-Activated Cell Sorting of CD133<sup>+</sup> and CD133<sup>-</sup> MB cells

CD133<sup>+</sup> MB cells were labeled with phycoerythrin (PE)-conjugated monoclonal antibodies against human CD133 (CD133/2-PE, Milteny Bio) at 4°C for 10 minutes per manufacturer's instructions, as we described previously.<sup>35</sup> Cells were then washed and resuspended in a stem cell growth medium consisting of Neurobasal media (Invitrogen), N2 and B27 supplements (0.5× each; Invitrogen), human recombinant bFGF and EGF (50 ng/mL each; R&D Systems),<sup>34</sup> penicillin G, and streptomycin sulfate (1:100; GIBCO-Invitrogen). CD133<sup>+</sup> and CD133<sup>-</sup> cells were then flow-sorted with Cytomation MoFlo (Dako). Dead cells were excluded by propidium iodide (PI) staining.<sup>35</sup>

#### In Vitro Analysis of Viral Infection

Fluorescence-activated cell sorting (FACS)-purified CD133<sup>+</sup> and CD133<sup>-</sup> cells were seeded at 8000 cells/well in 24-well plates and cultured overnight before being treated with SVV-GFP at 2000 MOI for 48 hours. SVV-GFP infectivity was then determined through flow cytometry analysis in duplicate by examining the intracellular expression of GFP. Dead cells were excluded by PI staining and cell debris gated out using the forward high scatter setting.

#### Neurosphere Assay

Single-cell suspensions prepared from xenograft tumors were plated in clonal density (1500 cells/100 μL) and incubated in CSC medium consisting of Neurobasal media, N-2 and B-27 supplements (0.5× each; Invitrogen), and human recombinant bFGF and EGF (50 ng/mL each; R&D Systems), as well as penicillin G and streptomycin sulfate (1:100; Invitrogen), for

14 days.<sup>34,35</sup> The suppression of neurosphere growth was examined with CCK8 assay.

#### In Vivo Treatment

SVV-001 (5 × 10<sup>12</sup> vp/kg) was diluted with PBS and administered through a single tail vein injection in 2 different MB models at 2 and 4 weeks, respectively, post-tumor injection (*n* = 10 per group). Body weights were monitored weekly as a surrogate indicator of SVV-001 systemic side effects. Mice that developed neurological deficits were euthanized and their brains removed for histopathological analysis. Mice receiving injection of PBS (*n* = 10) were included as controls. To study the biological changes caused by SVV-001, we allowed the injected xenograft cells in a separate group to grow for ~8 weeks to form tumors 8–12 mm in diameter before being treated with SVV-001 as described above. Mouse brains were then removed at 1, 2, and 6 days after virus injection and analyzed.

#### Immunohistochemical Staining

This was performed using a Vectastain Elite Kit (Vector Laboratories) as described previously.<sup>37</sup> Primary antibodies included mouse antibody to SVV-001 capsid protein (2A9) (1:200; Neotropix), human mitochondria (MT) (1:50; Abcom), LC3 (1:100), and caspase 3 (1:100; Santa Cruz). Antigen retrieval was performed in a pressure cooker in 0.03 M sodium citrate acid buffer. After the slides were incubated with primary antibodies, the appropriate biotinylated secondary antibodies (1:200) were applied, and the final signal was developed using the 3,3'-diaminobenzidine substrate kit for peroxidase.

#### Treatment with Autophagy Activator and Inhibitors

Tumor cells were plated in 96-well plates and pretreated with the autophagy activator rapamycin (10 μM; Sigma-Aldrich) and inhibitors, including 3MA (10 mM), vinblastine (10 ng/mL), pepstatin A (100 μM), and bafilomycin A1 (200 nM; Sigma-Aldrich), for 24 hours before SVV-001 at an MOI of 1 was added. Cell viabilities

were checked with the cell-counting kit 7 days after SVV-001 treatment.

### Western Hybridization

Primary cultured cells were treated with SVV-001, alone or in combination with 3MA (autophagy inhibitor) or rapamycin (autophagy activator), for 24 hours. Cell proteins were extracted and separated in a 4%–20% sodium dodecyl sulfate–polyacrylamide gel electrophoresis, transferred to polyvinylidene fluoride membrane using standard methods, and incubated with the following primary antibodies: LC3B (1:100), beclin (1:100), Atg5 (1:500), Atg7 (1:500), and Atg12 (1:500) (Cell Signaling), poly(ADP-ribose) polymerase (PARP) (1:500; Sigma), and caspase 3 (1:200; Santa Cruz). After the blots were incubated with enzyme-linked secondary antibody (horseradish peroxidase), chemiluminescent detection reagents (Amersham) were used to reveal results.

### Quantitative Reverse Transcription–PCR

Quantitative analysis of extracellular viral production was performed with SYBR green master mix in an ABI 7000 DNA detection system (Applied Biosystems), as we described previously.<sup>36</sup> Complementary DNA was synthesized with MuLV reverse transcriptase (RT) and random hexamers (PerkinElmer) in a total volume of 20  $\mu$ L from 5  $\mu$ L of cell-free culture media. Primers for PCR amplification were designed to flank more than 1 exon (forward: 5'-TGGTGGTCCTTAGAGGC AAG; backward: 5'-AAATCTGGATCTGGGGGAAG). Expression levels of selected genes were normalized to the SVV-001 standard that contained  $10^7$  vector particles (vp) using the  $\Delta\Delta$  cycle threshold (Ct) method.

### Statistical Analysis

In vitro cytotoxic effects and changes in viral production were analyzed through 1-way analysis of variance followed by pairwise multiple comparisons with the Tukey test; and differences in animal survival times were subjected to a log-rank analysis using SigmaStat (Systat Software). The data were plotted with SigmaPlot (Systat Software). *P*-values of  $<.05$  were considered statistically significant for all tests.

## Results

### SVV-001 Kills Primary Cultured MB Xenograft Tumor Cells

To determine if SVV-001 could infect and kill MB cells, we treated primary cultured xenograft cells derived from the 10 primary tumor-based orthotopic xenograft mouse models<sup>35</sup> with SVV-001 ranging from 0.3 to 66 MOI for 72 hours. A reduction in cell viability was detected in 5 of the 10 tumors, including 4 anaplastic MBs and 1 classic MB (Fig. 1A). The minimum MOI

of SVV-001 required to produce statistically significant growth suppression ranged from 0.3–0.4 (ICb-1299MB, ICb-1572MB, and ICb-1078MB) to 3.6–4.4 (ICb-984MB and ICb-1487MB). Proliferation of the remaining 5 tumors (1 classic MB model ICb-1192MB, 2 nodular MB models ICb-1338MB and ICb-1197MB, and 2 anaplastic MB models ICb-1494MB and ICb-1595MB) was not affected by SVV-001 (MOI: 25–50; Fig. 1A). To examine whether the suppressed cell proliferation was the result of cell death, we used the MTT assay to directly visualize live cells in situ by microscopic examination of the blue intracellular crystal formation. A remarkable reduction in viable cells was observed in all the permissive but not the resistant tumor cells (Fig. 1B).

### SVV-001 Effectively Infects CD133<sup>+</sup> MB Cells

Given the critical roles of CSCs in therapy resistance and tumor recurrence,<sup>8–12</sup> it is important to determine whether SVV-001 can eliminate MB stem cells. However, our understanding of CSCs in MB is incomplete, and there is currently no single marker that can reliably identify all the MB stem cells. Since CD133 has been successfully used to characterize and isolate at least a subpopulation of CSCs in MB,<sup>3,5,35</sup> we examined whether CD133<sup>+</sup> MB cells were equally susceptible to SVV-001 as the CD133<sup>-</sup> MB cells in the permissive models. We used SVV-GFP, the genetically modified SVV-001 that has a high particle-to-infectivity ratio compared with natural SVV-001 to infect FACS-purified CD133<sup>+</sup> and CD133<sup>-</sup> cells derived from 5 orthotopic models that displayed different permissiveness. In the permissive models treated with SVV-001 for 48 hours, effective infection was observed in the CD133<sup>+</sup> cells, resulting in 62.8% positivity in the ICb-1299MB, 23.4% in the ICb-1078MB, and more than 10% in the ICb-984MB; whereas in the resistant tumors (ICb-1494MB and ICb-1595MB), less than 5% SVV-GFP positivity was observed ( $P < .05$ ; Fig. 2A and B). The levels of SVV-GFP infectivity in the CD133<sup>-</sup> tumor cells were similar to those observed in the corresponding CD133<sup>+</sup> cells ( $P > .05$ ), with high-level GFP positivity found in the permissive tumors and low positivity in the resistant models (Fig. 2A and B). These data showed that both CD133<sup>+</sup> MB stem cells and CD133<sup>-</sup> cells can be effectively infected by SVV-001, suggesting that the CSC status of CD133<sup>+</sup> MB cells does not block the infectivity of SVV-GFP.

### SVV-001 Kills CSCs and Consequently Prevents Neurosphere Formation

There is recent evidence suggesting that not all brain tumor CSCs are CD133<sup>+</sup>. Other cell surface markers (such as CD15, CD44, and CD24) and phenotypic features, such as ALDH1, have also been associated with human CSCs.<sup>38–46</sup> Therefore, demonstrating the infectivity of SVV-GFP on CD133<sup>+</sup> MB cells is necessary but may not be sufficient to prove that SVV-001 can kill all MB stem cells. We then utilized the



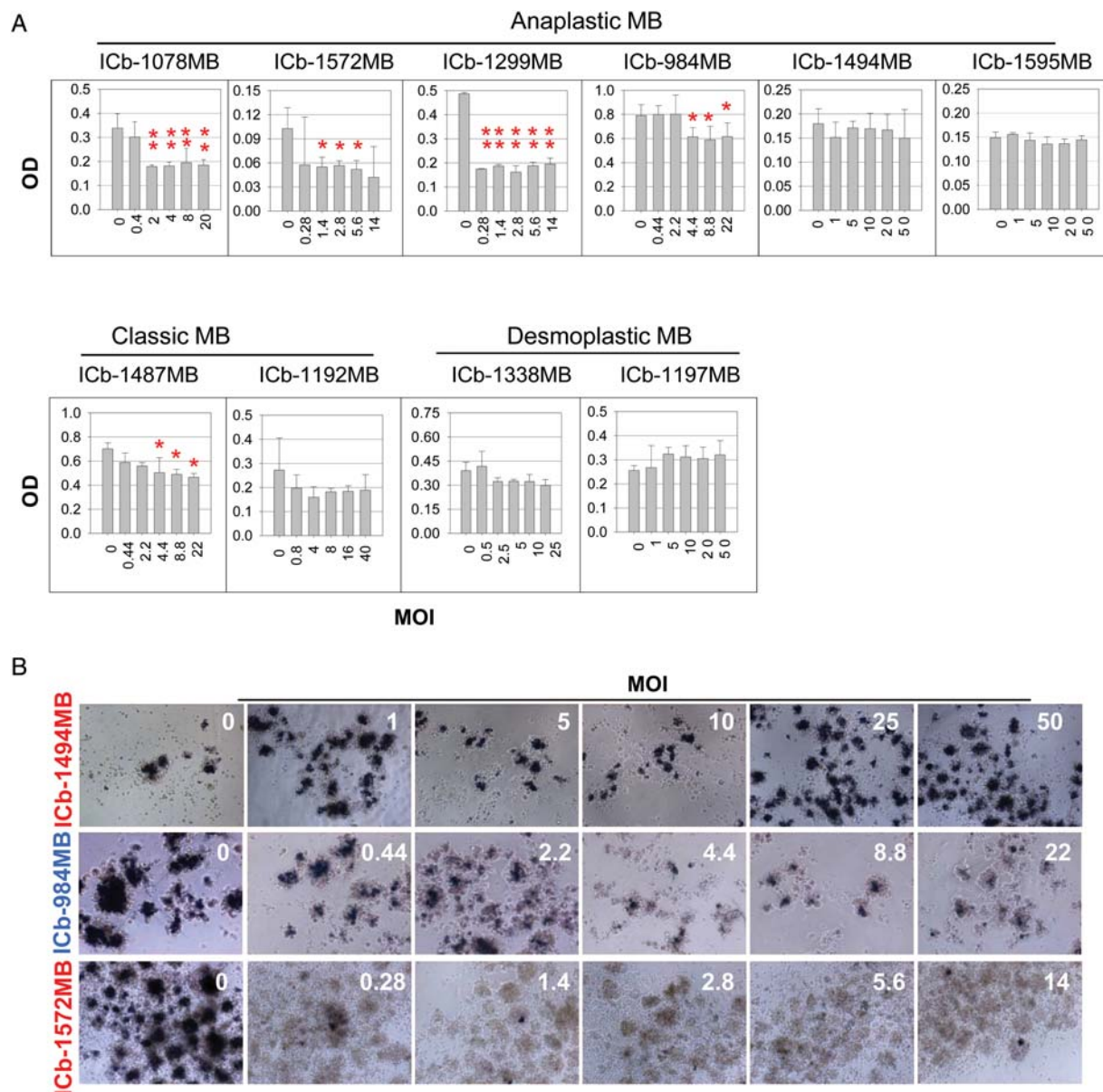


Fig. 1. Suppression of primary cultured MB xenograft tumor cells with SVV-001. (A) Quantitative assessment of cell proliferation (mean  $\pm$  SD) with a CCK8 assay. After cells were exposed to SVV-001 for 72 hours, assessment indicates 4 anaplastic and 1 classic MB were successfully infected ( $*P < .05$  and  $**P < .01$ ). (B) Representative images show the changes of cell viability in the resistant (ICb-1494MB) and permissive (ICb-984MB and ICb-1572MB) models as detected with an MTT assay (magnification  $\times 10$ ). Compared with the control and resistant models (ICb-1494MB) in which the formation of dark blue intracellular crystals was evident, there was a significant decrease and loss of the stained viable cells in the permissive models ICb-984MB and ICb-1572MB, respectively.

neurosphere assay, a functional assay that is used to identify normal and cancerous stem cells by examining their exclusive capabilities of self-renewal regardless of the cell surface markers,<sup>3,5,35</sup> to examine whether SVV-001 can kill the MB cells that possess this critical feature of CSC. Freshly prepared single-cell suspensions derived from the 5 permissive models were plated at clonal density in the serum-free medium that favors the growth of CSCs<sup>35</sup> and treated with SVV-001 (0.5–25 MOI). Compared with the mock-treated cells, in which the formation of neurospheres

was evident by day 14, suppression or near complete prevention of neurospheres was observed in all 5 permissive models ( $P < .001$ ) (Fig. 2C). Further examination with an MTT assay confirmed the absence of viable cells in the residual neurospheres treated with SVV-001 (Fig. 2D), and we were therefore unable to examine their capabilities of forming second and third generations of neurospheres. This result provided additional evidence to support the notion that SVV-001 is capable of targeting MB cells that exhibit critical stem cell features.

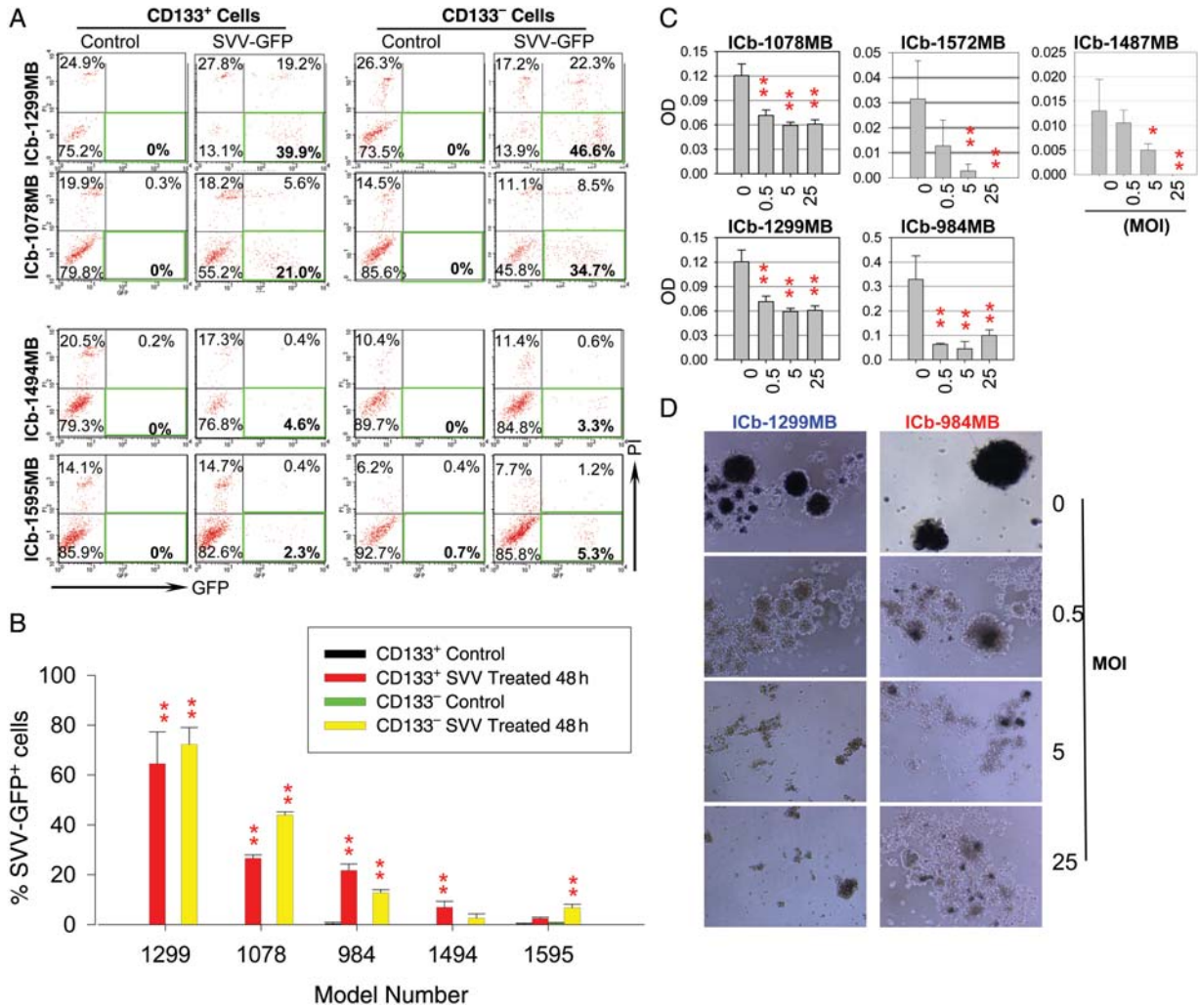


Fig. 2. Intracellular replication of SVV-GFP in FACS-purified CD133<sup>+</sup> cells, and suppression of neurosphere formation from single CSCs. (A) Representative graph showing the high-level infection of CD133<sup>+</sup> and CD133<sup>-</sup> cells by SVV-GFP (MOI of 2000 for 48 hours) in the 2 permissive models (ICb-1299MB and ICb-1078MB) compared with the 2 resistant models (ICb-1494MB and ICb-1595MB). (B) Quantitative analysis of SVV-GFP<sup>+</sup> cells with flow cytometry showing the high (ICb-1299MB and ICb-1078MB) and medium level (ICb-984MB) positivity in both the CD133<sup>+</sup> and the CD133<sup>-</sup> cell fractions in the permissive tumors compared with the low positivity in the resistant tumors (ICb-1494MB and ICb-1595MB) (\*\*P < .01 compared with the control cells.) (C) Suppression of the neurosphere forming capability of SVV-001 in the 5 permissive models as determined with a CCK8 assay (\*P < .05, \*\*P < .01). (D) Representative images showing the inhibition of neurosphere formation from single MB cells 14 days post-SVV-001 (0–25 MOI) treatment in vitro in 2 permissive models using an MTT assay. Only viable cells in the mock-treated control groups were able to convert MTT into dark blue intracellular crystals.

*Systemically Administered SVV-001 Can Pass the BBB to Infect and Replicate in Intracerebellar Xenograft Tumor Cells Causing Widespread Cell Lysis*

Effective delivery of therapeutic agents into brain tumors are often impaired by the BBB. To determine whether SVV-001 can pass through the BBB and infect orthotopic xenograft tumors in mouse brain, we injected SVV-001 viruses ( $5 \times 10^{12}$  vp/kg) through tail veins into mice bearing large ICb xenografts (~ 8–12 mm in diameter on paraffin sections) of 2 permissive models (ICb-1299MB and ICb-1572MB) and examined the time-course (24 hours, 48 hours, and 6 days) and

spatial penetration of SVV-001 by immunohistochemical (IHC) staining of SVV-001 capsid protein (Fig. 3). To enable comprehensive analysis of tumor/host responses, the whole mouse brains were serially sectioned and processed for histopathological analysis.

In both models, patches of positively stained tumor cells were detected 24 hours after SVV-001 injection. Within these patches, the infected tumor cells were mostly surrounding a blood vessel, indicating that the viruses entered tumor parenchyma from the blood supply. These patches expanded in a starburst pattern over time. In ICb-1299MB (Fig. 3B), areas of the infected tumor cells started to merge by 48 hours, covering nearly half of the

tumor masses; and the infected tumor cells began to show early signs of nuclear condensations. By day 6, the SVV-001 penetration extended from the tumor core into invasive and metastatic foci. Highly condensed or fragmented nuclei and pink cytoplasmic inclusions became clearly visible. In the ICB-1572MB model (Fig. 3C), SVV-001's infection and penetration were even more potent. At 48 hours, more than 75% of the tumor cells in the core area and nearly all the cells in the invasive foci and cerebrospinal fluid spread were infected. Similar to those of ICB-1299MB, even the microinvasive satellites and infiltrating single tumor cells in the normal mouse brains in the ICB-1572MB xenografts were infected.

#### *A Single i.v. Injection of SVV-001 Significantly Prolonged Animal Survival Times*

To determine the therapeutic efficacy and establish preclinical rationale of SVV-001 for MBs, we examined the impact of i.v. injected SVV-001 on animal survival times in the 2 most aggressive anaplastic MBs (ICB-1299MB and ICB-1572MB) that were susceptible to SVV-001-induced cell killing in vitro. These 2 models are also shown to have replicated the histopathological, invasive growth, and genetic features of the original patient tumors and preserved the CD133<sup>+</sup> CSCs in vivo (10% in ICB-1299MB [at passage 3] and 1.5% in ICB-1572MB [at passage 4]).<sup>35</sup> Mice receiving ICB engraftment of tumor cells ( $1 \times 10^5$ /mouse) from the same passage of these 2 permissive MBs were allowed to grow for 2 and 4 weeks to form small-sized (~1 mm) and medium-sized (3–4 mm) tumors (determined on serial paraffin sections),<sup>35</sup> respectively, before being treated with a single tail vein injection of SVV-001 ( $5 \times 10^{12}$  vp/kg). This treatment significantly improved the survival in both models. For ICB-1299MB (Fig. 4A), the survival fraction increased from 0% in the untreated group to 20% in both of the treated groups after 264 days of observation. The median survival time increased from  $63.8 \pm 4.2$  days in the saline-treated control group to 2.2 times longer ( $141.6 \pm 25.2$  days) in mice bearing small tumors ( $P < .00001$ ) and 2.9 times longer ( $187.9 \pm 20.3$  days) in mice bearing medium-sized tumors ( $P < .001$ ). For ICB-1572MB (Fig. 4A), the survival fraction and times, which were 0% and  $40.2 \pm 3.4$  days in the untreated group, were 40% and  $239 \pm 11.5$  days (5.9-fold) in mice with small tumors ( $P < .00001$ ), and 20% and  $159.3 \pm 22.9$  days (3.96-fold) in mice with medium-sized tumors ( $P < .0001$ ). Survival times in mice with small vs medium-sized tumors were not significantly different in the ICB-1299MB model ( $P = .447$ ), whereas mice bearing small ICB-1572MB tumors survived longer ( $P < .05$ ) than their counterparts bearing larger tumors, suggesting that the impact of tumor size on responsiveness is variable.

#### *SVV-001 Eliminates Preformed MB Xenograft Tumors In Vivo*

The CSC theory suggested that CSCs have to be eradicated for a cure.<sup>12,13</sup> Therefore, complete eradication of

preformed xenograft tumors that are known to have preserved human CSCs should serve as a critical and reliable, albeit indirect, indicator of CSC elimination. This is particularly important for MBs, since our understanding of MB stem cells is still incomplete and not all MB markers have been properly defined. To determine whether SVV-001 completely eliminated preformed MB xenografts, we analyzed serial sections of paraffin-embedded whole mouse brains of the 10 long-term survivors that were euthanized at day 264. Only the 2 ICB-1299MB mice bearing medium-sized xenografts at treatment were found to have small-sized (~2.5 mm) and medium-sized (4 mm) residual tumors (Fig. 4B). In the remaining 8 mice, no residual tumor was detected (Fig. 4B). Signs of disturbed granular layer cells, which are indicative of previous injection or tumor growth, and some micronodules of foamy cells with a condensed nucleus and vacant cytoplasm were found (Fig. 4C). IHC using human-specific antibodies to mitochondria did not detect positive cells in the 8 xenografts (Fig. 5C), providing direct evidence of complete tumor elimination.

#### *SVV-001-Induced Cell Killing Is Restricted to MB Tumor Cells*

Previous studies have shown that none of the 17 normal primary human cells, including fetal cortical neurons and adult astrocytes, were infected when exposed to high MOI ( $>10,000$ ).<sup>29</sup> To examine the toxicity of SVV-001 to RAG2/SCID mice, we monitored animal body weights weekly for 8 weeks and examined the mice daily for signs of sickness, including slow movement and hunched postures. Despite some variations, none of the mice was found to have lost more than 20% of its body weight. Further histopathological examination of mouse brains showed that SVV-001 did not infect any adjacent cerebellar granular neurons or glial cells or cells in the cerebral grey or white matter. Viral capsid proteins were also absent in the ventricles, blood vessels, and tumor-free subarachnoid spaces (Figs 3 and 4), indicating that SVV-001 selectively infects human MBs while sparing normal mouse brain cells.

#### *SVV-001 Viruses Activated Autophagy Both In Vitro and In Vivo*

Cellular autophagy has been hypothesized to mediate viral replication for several positive-stranded RNA viruses.<sup>47,48</sup> To determine whether SVV-001 activated autophagy, we examined the changes of an autophagy marker (LC3B) and key autophagy regulators (beclin, the Atg5/Atg12 conjugate, and Atg7) in vitro in cells derived from 1 resistant and 1 permissive MB xenograft model (Fig. 5A). Western hybridization showed that exposure to SVV-001 at 25 MOI for 24 hours induced the conversion of LC3B from type I to type II in the permissive model ICB-1299MB, but not in the resistant model (ICB-1595MB (Fig. 5B) in which the autophagy



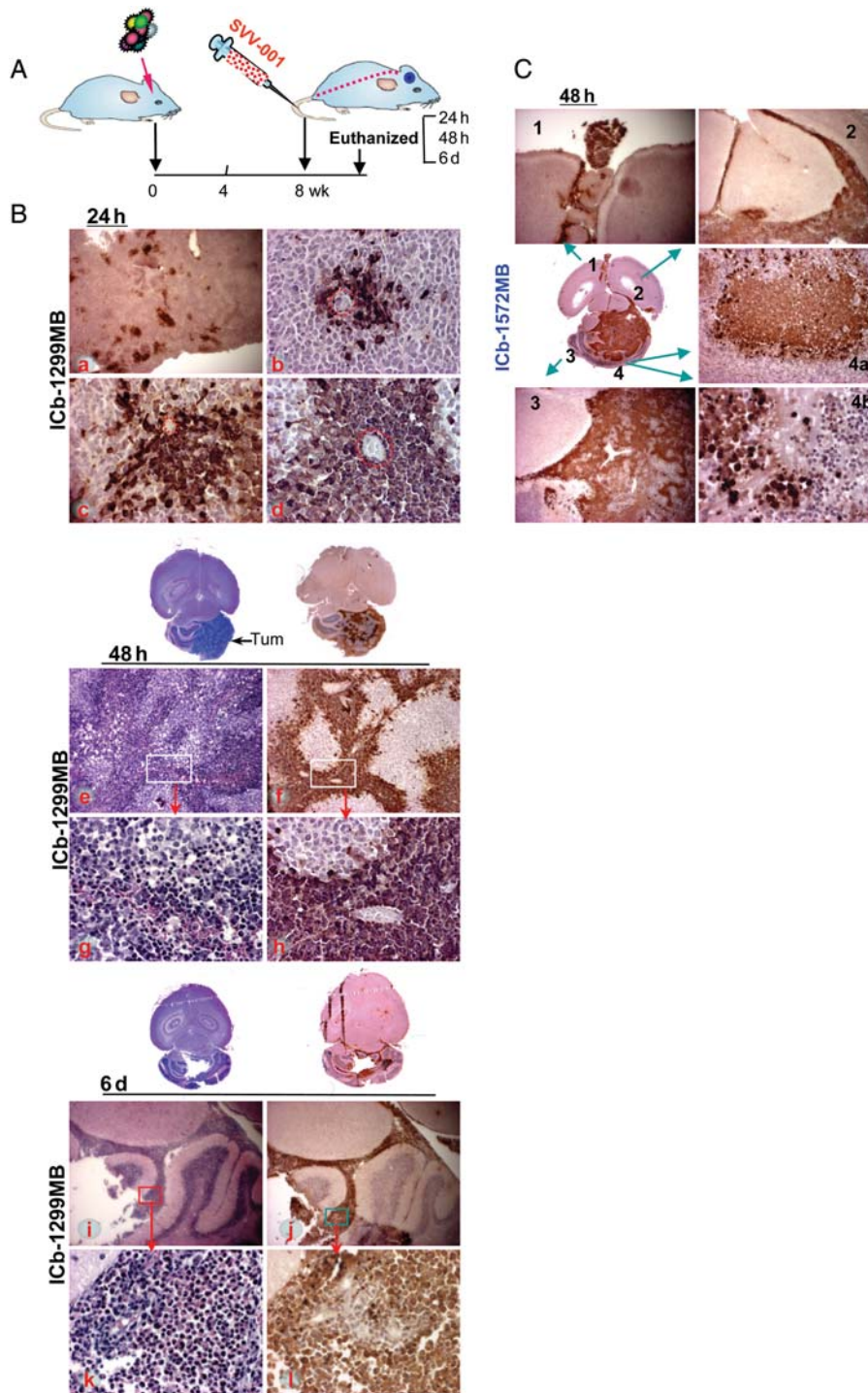


Fig. 3. In vivo infectivity and killing of MB xenograft cells induced by SVV-001. (A) Overview of the experimental design. SVV-001 ( $5 \times 10^{12}$ vp/kg) was administered through a single tail vein injection. Mice ( $n = 2-3$  per test) were then euthanized at predetermined time points (24 hours, 48 hours, and 6 days). (B) Time-course infectivity of SVV-001 in Icb-1299MB at 24 hours (a–d), 48 hours (e–h), and 6 days (i–l). Infection of xenograft tumor cells by SVV-001 was determined with IHC staining using mouse antibodies against SVV-001 capsid protein (2A9) (a–d, f, h, j, and l) and compared with the corresponding hematoxylin and eosin staining (e, j, i, and k). Dotted lines in b and d encircle microvessels. Note the pink cytoplasmic inclusions in k. (C) Selective spatial infectivity of SVV-001 in Icb-1572MB 48 hours after virus injection. SVV-001 infected not only the tumor mass (C3), but also the cells spread through cerebrospinal fluid (C1 and C2), as well as an invasive nodule (C4a) and nonvascularized single tumor cells (C4b) while leaving normal mouse brain cells (C1–C3), even those in close proximity to tumor cells (C4b), unharmed. Magnifications:  $\times 4$  (a, i, j, C1, C3),  $\times 10$  (e, f, C4a), and  $\times 40$  (b–d, g, h, k, l, C4b).



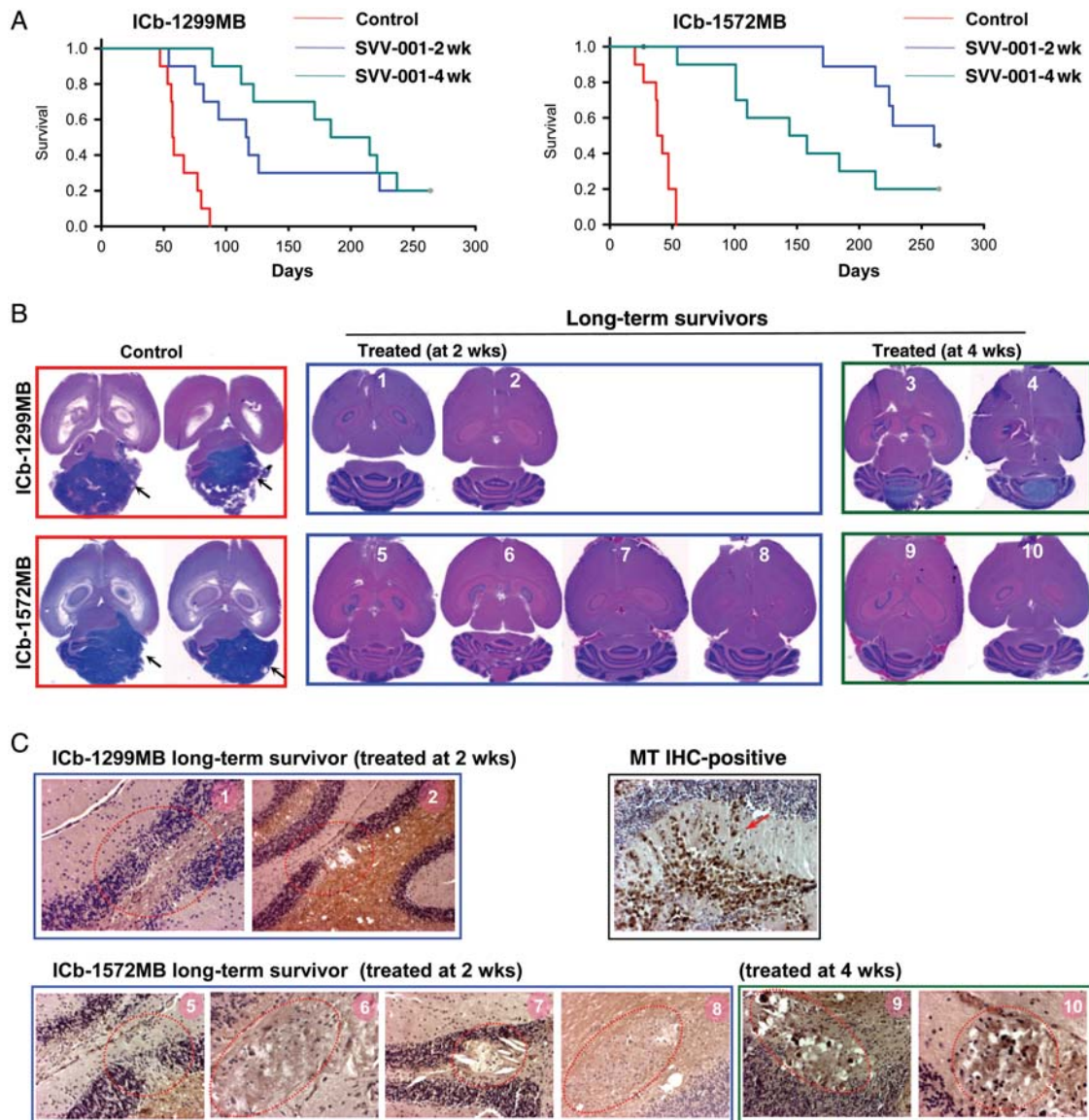


Fig. 4. Prolongation of animal survival times and elimination of preformed xenograft tumors. SVV-001 ( $5 \times 10^{12}$  vp/kg) was administered through a single tail vein injection 2 and 4 weeks after tumor cell transplantation ( $n = 10$  per group). (A) Log-rank analysis of animal survival times showing significant improvement of animal survival times in mice treated with SVV-001 ( $P < .01$ ). (B) Hematoxylin and eosin (H&E) staining of paraffin sections showing elimination of xenograft tumors in 8 of the 10 long-term survivors, compared with the huge ICb MB xenografts in the mock-treated control groups (arrow). (C) IHC staining with human-specific antibodies against mitochondria in the 2 ICb-1299MB (mice #1 and #2) and 6 ICb-1572MB (mice #5–10) mice in which no residual tumors were observed with H&E staining. Compared with the intense positivity (arrow) detected in the positive control section, no MT-positive cells were detected in the 8 brains, though a disturbance of the granular layer and micronodules with empty/shallow cytoplasm and condensed nuclei (circled in red) were seen. Magnification:  $\times 40$ .

activator rapamycin successfully converted LC3B from type I to type II (Fig. 5B). In the permissive cells, expression of beclin, Atg5/Atg12, and Atg7 were not altered, whereas in the resistant cells, increased Atg12 alone was observed.

We then determined whether SVV-001 also activated autophagy in vivo by examining the expression of the autophagy marker LC3 in the 2 MB xenografts (ICb-1299MB and ICb-1572MB) 48 hours after SVV-001 intravenous injection (Fig. 5C). In both

models, the expression pattern of LC3B closely mirrored that of the SVV-001 capsid protein expression: the strongest staining was found in the front edge of infected cells of ICb-1299MB and in islands of strong positive cells of ICb-1572MB. The noninfected tumor cells were negative (Fig. 5C), suggesting that SVV-001 replication and subsequent cell killing were mediated through the induction of autophagy.

To examine whether apoptosis also played a role, we reprobated the same western blots with antibodies to

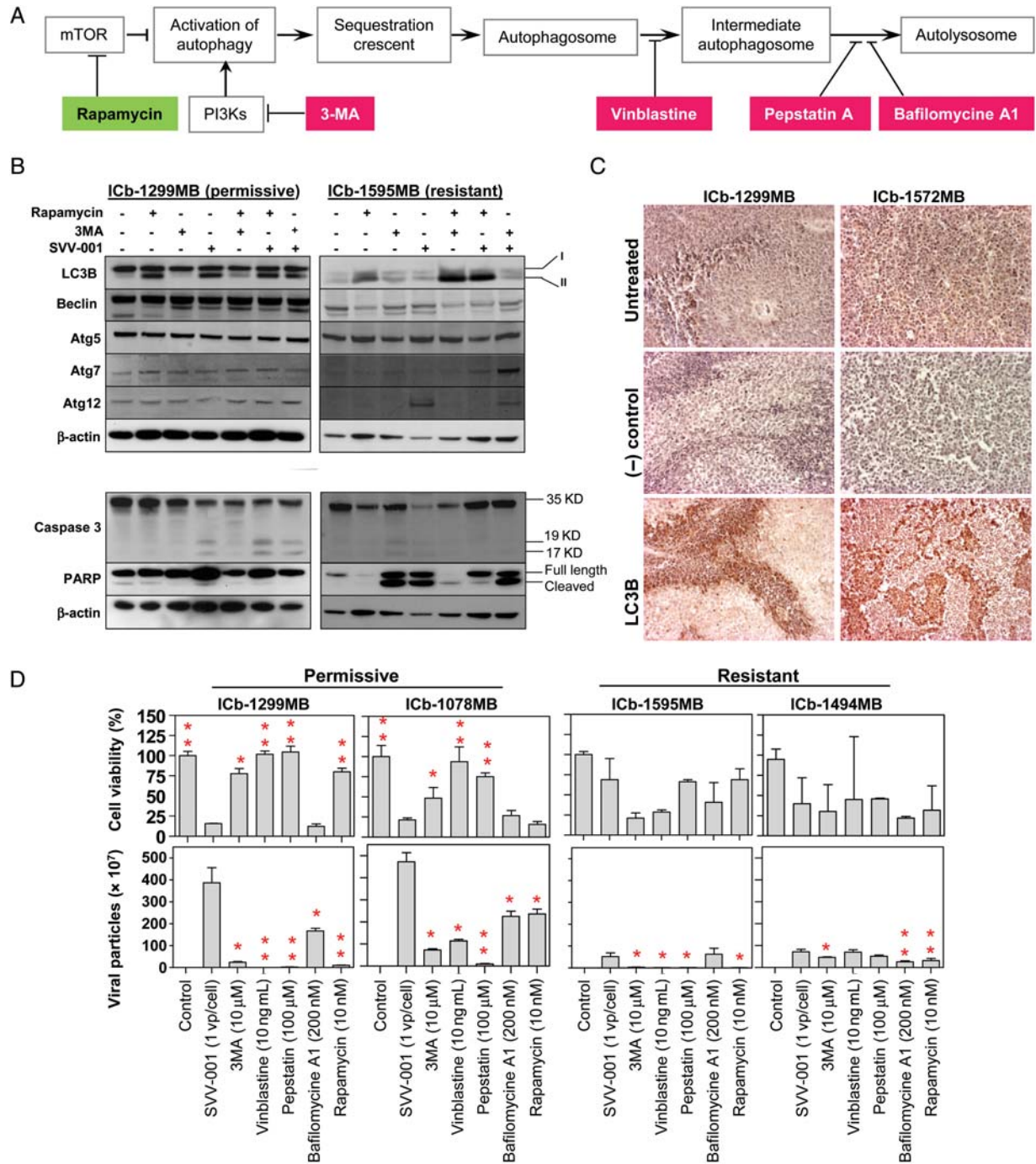


Fig. 5. Induction of autophagy and apoptosis by SVV-001. (A) Overview of the steps activating autophagy and the specific activator. (B) Changes of autophagy (upper panel) and apoptosis (lower panel) genes induced by SVV-001 in vitro. Primary cultured cells from the permissive model ICb-1299MB and the resistant model ICb-1595MB were treated with SVV-001 (MOI 25) for 24 hours before being subjected to western hybridization. The autophagy inducer rapamycin (10 nM) and inhibitor 3MA (10  $\mu$ M) were also included as controls. (C) IHC detection of LC3B expression in vivo in the 2 permissive xenograft mouse models 48 hours after SVV-001 single tail vein injection. (D) Impact of autophagy inhibitors (3MA, vinblastine, pepstatin, and bafilomycin A1) and activator (rapamycin) on the cell killing (upper panel) and extracellular viral production (lower panel). Cell viabilities in cells treated with combined drug (inhibitor or activator) and SVV-001 were normalized to those treated with drug only and presented as percentages. Treatment with autophagy inhibitors led to increased cell viability in the permissive models (upper panel) and decreased extracellular viral production in both the permissive and resistant models (\* $P$  < .05 and \*\* $P$  < .01 when compared with SVV-001 only) (lower panel).



PARP and caspase 3 (Fig. 5B). Although SVV-001 induced cleavage of PARP in the resistant tumor ICb-1595MB, it failed to exert a similar effect in any of the permissive models. There were, however, low levels of cleaved caspase 3 in the ICb-1299MB tumor cells (Fig. 5B). In agreement with this finding, immunostaining on SVV-001-treated xenograft tumors *in vivo* revealed only scattered caspase 3-positive cells in ICb-1299MB and ICb-1572MB xenograft tumors 48 hours post-SVV-001 treatment, suggesting that apoptosis may not have played a major role.

#### *Inhibition of Autophagy-Protected Permissive MB Stem Cells by Suppressing SVV-001 Replication*

To further confirm the role of autophagy in SVV-001-induced cell killing, we applied the autophagy activator rapamycin and various inhibitors<sup>49</sup> to preformed neurospheres derived from 2 permissive (ICb-1299MB and ICb-1078MB) and 2 resistant MB xenograft models (ICb-1595MB and ICb-1494MB). The cell viability was examined 7 days post-SVV-001 (MOI of 1) infection to give the viruses more than enough time to infect and kill the target cells. In the 2 permissive models, treatment with autophagy inhibitors targeting sequestration (3MA), lysosomal fusion (vinblastine), and lysosomal enzymes (pepstatin A) significantly protected the MB stem cells from SVV-001-induced killing, though bafilomycin A1, an inhibitor of a vacuolar-type ATPase that inhibits the formation of autolysosome, failed to block the cell-killing effects of SVV-001 (Fig. 5D). In the 2 resistant models, addition of 3MA and vinblastine did not provide the similar protection but caused reduced cell viability, particularly in ICb-1595MB (Fig. 5D).

Since treatment with the autophagy activator rapamycin did not sensitize resistant cells to SVV-001 and had little effect on the permissive models (Fig. 5B), we reasoned that SVV-001 activates autophagy to complete its intracellular replication rather than relying on autophagy to kill the target cells. To test this hypothesis, we utilized quantitative RT-PCR to quantitate the total viral particles (dead and live) that were released into culture media in the 2 permissive and 2 resistant models. The cells were treated with SVV-001 (MOI of 1) and/or autophagy activator/inhibitors as described above for 7 days without passaging, so that the viruses had sufficient time to lyse the infected tumor cells after intracellular replication and to release the progeny virions into the culture media. Our results showed that viral particles of SVV-001 in the culture media of permissive models (ICb-1078MB and ICb-1299MB) were significantly higher than those in the resistant models (ICb-1494MB and ICb-1595MB) ( $P < .001$ ) and that treatment with autophagy inhibitors (3MA, vinblastine, pepstatin A, and bafilomycin A1) for 7 days significantly suppressed the viral yields in all 4 models, though the effects were much more prominent in the permissive tumors than in the resistant models ( $P < .05$ ) (Fig. 5D). Moreover, we observed a reverse correlation

between the decrease in viral production and the increase in cell viability in the 2 permissive models ( $r = -.51$  and  $-.82$  in ICb-1078MB and ICb-1299MB, respectively), further supporting the role of autophagy in SVV-001 replication.

#### *Rapamycin Did Not Sensitize the Resistant MB Cells to SVV-001*

Rapamycin, an inhibitor of mTOR, was shown to enhance the oncolytic activity of myxoma virus and increase coxsackie virus replication.<sup>21,50</sup> Since it also activates cellular autophagy, we set to examine if rapamycin enhances the cell killing and intracellular replication of SVV-001 in MBs, particularly in the resistant cells. *In vitro* treatment with rapamycin (10 nM) for 24 hours resulted in the conversion of LC3B from type I to type II in both the permissive (ICb-1299MB) and the resistant (ICb-1595MB) cells (Fig. 5B), indicating that rapamycin indeed activated the cellular autophagy in these cells. Combining rapamycin with SVV-001, however, did not enhance its cell-killing effects or increase extracellular viral production (Fig. 5D). Since rapamycin alone significantly suppressed cell proliferation in the permissive ICb-1078MB (>80%) and the resistant ICb-1494MB (>75%) ( $P < .001$ ), models the less viable cells appeared to have partially played a role in the low-level viral production. In the remaining 2 models, the permissive ICb-1299MB and the resistant ICb-1595MB, the suppressive effects of rapamycin on cell proliferation were minimal. Still the viral productions were not increased (Fig. 5D), suggesting that rapamycin cannot be used to increase the responsiveness of MB cells toward SVV-001. Although the detailed mechanism of intracellular replication of SVV-001 remains elusive, previous studies have shown that some RNA viruses, such as poliovirus and rhinovirus, subvert the components of the autophagy machinery for viral replication by using the surface of double-membraned cytoplasm as the site of viral RNA replication.<sup>51</sup> Since autophagy can serve in the innate immune response to microorganisms, our finding that rapamycin did not increase SVV-001 replication suggests that the activated autophagy by rapamycin in our MB models was not identical to that induced by SVV-001, and the rapamycin-activated autophagy may have interfered with the autophagic component(s) that are needed by SVV-001 for intracellular replication.

## Discussion

Here, we show that the oncolytic picornavirus SVV-001 possesses strong antitumor activities against human MBs. We demonstrated that SVV-001 infected and killed MB cells, including the CD133<sup>+</sup> cells and the cells that can form neurospheres, *in vitro*. More importantly, we demonstrated that a single tail vein injection of SVV-001 can pass through BBB and eliminate pre-established MB xenografts *in vivo*, leading to long-term tumor-free survival in a subset of primary tumor-based orthotopic mouse models. Our mechanistic



study further showed that SVV-001 activated autophagy, albeit not identical to that triggered by the known autophagy activator rapamycin, for intracellular replication.

Since our data were obtained through a relatively large panel of primary tumor-based xenograft models that have been shown to faithfully reproduce genetic and clinical phenotypes of the original MBs,<sup>3,5</sup> our results may have a high clinical predictive value. The high (67%) response rate in anaplastic MB models suggests that this group of MBs, which are biologically more aggressive than classic and desmoplastic subtypes, may be an appropriate histological subtype to be prioritized for future clinical trials. Indeed, our results showed that the systemically administered SVV-001 effectively infected not only the tumor cells in the core area of tumor mass, but also the microscopic invasive cells and metastatic foci. Such characteristics, which have rarely been described before, represent a significant advantage of SVV-001 in targeting highly invasive/metastatic brain tumors.

In addition to killing differentiated MB xenograft cells as observed in the primary cultures, our study also suggested that the eradication of MB stem cells by SVV-001 might have played a role in the elimination of orthotopic xenograft tumors. We first showed that SVV-001 effectively infected CD133<sup>+</sup> MB cells. We and others have shown that the CD133<sup>+</sup> MB cells possess key stem cell features, including self-renewal and multilineage differentiation, and have participated in the formation of serially transplantable xenografts.<sup>3,5,35</sup> Although recent studies have indicated that not all brain tumor stem cells are CD133<sup>+</sup>, and new markers such as CD15 have been described,<sup>38,41,52,53</sup> there is no report disqualifying CD133 as a marker for at least a subpopulation of brain tumor stem cells. Recognizing the limitations of cell surface markers for CSCs, we subsequently validated SVV-001's cell-killing activities against MB stem cells in the neurosphere assay.<sup>54,55</sup> Because this assay examines the *in vitro* self-renewal capacity, which is one of the most important features of CSCs, inhibition of neurosphere formation of MB cells in the serum-free medium supplemented with EGF and bFGF, which is shown to favor the growth of CSCs,<sup>3,55</sup> provided additional evidence to demonstrate the cell-killing activity of SVV-001 against MB stem cells. The final and most important support was provided by our *in vivo* finding that SVV-001 eliminated the preformed xenograft tumors in a subset of treated animals. Since the surviving mice were monitored for 264 days and the mock-treated mice all died within 90 and 60 days in ICb-1299MB and ICb-1572MB, respectively, it is reasonable to believe that the chance of tumor recurrence is minimal. Because CSCs have to be eliminated for a cure,<sup>12,13</sup> the long-term tumor-free survival provided strong preclinical evidence to demonstrate that SVV-001 has successfully eliminated not only CD133<sup>+</sup> MB stem cells but also other CSCs that may not be CD133<sup>+</sup> as well.

Autophagy is a cellular degradation pathway for the clearance of damaged or superfluous proteins and organelles.<sup>56</sup> It has also been shown to act as a defense mechanism against certain viruses.<sup>57–59</sup> In this study, we showed that SVV-001 induced conversion of LC3B from type I to type II, which is a marker of autophagy activation, and inhibition of autophagy protected MB cells from SVV-001 induced cell killing and reduced extracellular viral production. However, unlike adenovirus Delta-24-RGD, which induced upregulation of the Atg12/Atg5 complex in glioma stem cells,<sup>24</sup> SVV-001 did not alter the protein expression of Atg5/Atg12 or Atg7. This observation, combined with the fact that the autophagy activator rapamycin failed to increase SVV-001 replication in MB cells, seems to suggest that the autophagic machinery used by SVV-001 is not identical to bona fide autophagy.<sup>48</sup> The added activation of autophagy by rapamycin may have disturbed the autophagic process that is needed by SVV-001. Several other RNA viruses, such as influenza A virus<sup>60</sup> and poliovirus,<sup>61</sup> were shown to utilize membranes derived from the autophagic pathway to aid viral replication. It remains to be determined, however, whether SVV-001 depends on specific types or phases of autophagic membrane formation for viral production in MBs. Since low levels of caspase 3 activation and PARP cleavage were observed in the permissive cells, apoptosis does not appear to play a major role in SVV-001-induced cell killing.

The molecular mechanisms mediating the permissiveness of MB cells toward SVV-001 remain unknown. Although it is hypothesized that SVV-001 infects target cells through binding to cell surface receptors,<sup>29</sup> the complex mechanisms of oncolytic virotherapy elucidated to date suggest that identification of cellular surface markers predictive of clinical responses remains a significant challenge.<sup>62</sup> Therefore, testing a patient's resected MB specimen *ex vivo*, which takes only 3–7 days to complete, may provide critical information about its responsiveness to SVV-001. The strong correlation between *in vitro* and *in vivo* effects in our model system indicates that such an *ex vivo* approach may enable the preselection of cases appropriate for SVV-001 therapy.

One of the limitations of our current study is that the antitumor efficacy of SVV-001 was evaluated in immunodeficient animals. Therefore, potential additive or subtractive effects of host immune and inflammatory responses cannot be evaluated. Since SVV-001 viruses are replication competent and have a short replication cycle (<12 hours), it has the potential of producing effective cell killing before being cleared or neutralized by host immune responses. Previous studies have shown that SVV-001-specific antibodies usually did not become detectable until after 8 days after exposure in rodents and approximately 11 days in humans, but intratumoral replication of SVV-001 persisted for up to 14 days, despite high antibody titers, presumably as a result of sustained cell-to-cell infections that evaded circulating antibodies.<sup>29</sup> Recent studies have also shown that host immune mechanisms may also contribute to tumor eradication following administration of

oncolytic viruses.<sup>27,63</sup> Therefore, an intact host immune response may not necessarily interfere with SVV-001's infection and/or eradication of MB or other central nervous system tumors.

In summary, our data demonstrated the potent anti-tumor activities of SVV-001 against the pediatric brain tumor MB. We showed that SVV-001 can pass through the BBB and simultaneously eradicate both nonstem and stem MB cells to cause long-term tumor-free survival in patient-derived orthotopic xenograft mouse models. These findings suggest that SVV-001 is well suited to eliminate MBs and should be prioritized for the initiation of clinical trials. The capability of oncolytic viruses in targeting CSCs along with nonstem tumor cells may potentially be applied as a generalized

therapeutic strategy to safely and effectively eliminate human cancers so as to significantly improve clinical outcomes.

*Conflict of interest statement.* None declared.

## Funding

This work is supported by the Adrienne Helis Malvin Medical Research Foundation through its direct engagement in continuous active conduct of medical research in conjunction with Baylor College of Medicine and this program.

## References

- Geyer JR, Spoto R, Jennings M, et al. Multiagent chemotherapy and deferred radiotherapy in infants with malignant brain tumors: a report from the Children's Cancer Group. *J Clin Oncol.* 2005;23:7621–7631.
- Reya T, Morrison SJ, Clarke MF, Weissman IL. Stem cells, cancer, and cancer stem cells. *Nature.* 2001;414:105–111.
- Hemmati HD, Nakano I, Lazareff JA, et al. Cancerous stem cells can arise from pediatric brain tumors. *Proc Natl Acad Sci USA.* 2003;100:15178–15183.
- Singh SK, Hawkins C, Clarke ID, et al. Identification of human brain tumour initiating cells. *Nature.* 2004;432:396–401.
- Singh SK, Clarke ID, Terasaki M, et al. Identification of a cancer stem cell in human brain tumors. *Cancer Res.* 2003;63:5821–5828.
- Hope KJ, Jin L, Dick JE. Acute myeloid leukemia originates from a hierarchy of leukemic stem cell classes that differ in self-renewal capacity. *Nat Immunol.* 2004;5:738–743.
- Al Hajj M, Wicha MS, Benito-Hernandez A, Morrison SJ, Clarke MF. Prospective identification of tumorigenic breast cancer cells. *Proc Natl Acad Sci USA.* 2003;100:3983–3988.
- Bao S, Wu Q, McLendon RE, et al. Glioma stem cells promote chemoresistance by preferential activation of the DNA damage response. *Nature.* 2006;444:756–760.
- Creighton CJ, Li X, Landis M, et al. Residual breast cancers after conventional therapy display mesenchymal as well as tumor-initiating features. *Proc Natl Acad Sci USA.* 2009;106:13820–13825.
- Li X, Lewis MT, Huang J, et al. Intrinsic resistance of tumorigenic breast cancer cells to chemotherapy. *J Natl Cancer Inst.* 2008;100:672–679.
- Phillips TM, McBride WH, Pajonk F. The response of CD24(-/low)/CD44+ breast cancer-initiating cells to radiation. *J Natl Cancer Inst.* 2006;98:1777–1785.
- Eriksson M, Guse K, Bauerschmitz G, et al. Oncolytic adenoviruses kill breast cancer initiating CD44(+)CD24(-/low) cells. *Mol Ther.* 2007;15:2088–2093.
- Dingli D, Michor F. Successful therapy must eradicate cancer stem cells. *Stem Cells.* 2006;24:2603–2610.
- Wicha MS, Liu S, Dontu G. Cancer stem cells: an old idea—a paradigm shift. *Cancer Res.* 2006;66:1883–1890.
- Dean M, Fojo T, Bates S. Tumour stem cells and drug resistance. *Nat Rev Cancer.* 2005;5:275–284.
- Parato KA, Senger D, Forsyth PA, Bell JC. Recent progress in the battle between oncolytic viruses and tumours. *Nat Rev Cancer.* 2005;5:965–976.
- Liu TC, Kirn D. Targeting the untargetable: oncolytic virotherapy for the cancer stem cell. *Mol Ther.* 2007;15:2060–2061.
- Liu TC, Galanis E, Kirn D. Clinical trial results with oncolytic virotherapy: a century of promise, a decade of progress. *Nat Clin Pract Oncol.* 2007;4:101–117.
- Yang WQ, Senger D, Muzik H, et al. Reovirus prolongs survival and reduces the frequency of spinal and leptomeningeal metastases from medulloblastoma. *Cancer Res.* 2003;63:3162–3172.
- Cripe TP, Wang PY, Marcato P, Mahller YY, Lee PW. Targeting cancer-initiating cells with oncolytic viruses. *Mol Ther.* 2009;17:1677–1682.
- Lun XQ, Zhou H, Alain T, et al. Targeting human medulloblastoma: oncolytic virotherapy with myxoma virus is enhanced by rapamycin. *Cancer Res.* 2007;67:8818–8827.
- Lun X, Yang W, Alain T, et al. Myxoma virus is a novel oncolytic virus with significant antitumor activity against experimental human gliomas. *Cancer Res.* 2005;65:9982–9990.
- Marcato P, Dean CA, Giacomantonio CA, Lee PW. Oncolytic reovirus effectively targets breast cancer stem cells. *Mol Ther.* 2009;17:972–979.
- Jiang H, Gomez-Manzano C, Aoki H, et al. Examination of the therapeutic potential of delta-24-RGD in brain tumor stem cells: role of autophagic cell death. *J Natl Cancer Inst.* 2007;99:1410–1414.
- Wakimoto H, Kesari S, Farrell CJ, et al. Human glioblastoma-derived cancer stem cells: establishment of invasive glioma models and treatment with oncolytic herpes simplex virus vectors. *Cancer Res.* 2009;69:3472–3481.
- Kirn DH, Thorne SH. Targeted and armed oncolytic poxviruses: a novel multi-mechanistic therapeutic class for cancer. *Nat Rev Cancer.* 2009;9:64–71.
- Zhang Q, Yu YA, Wang E, et al. Eradication of solid human breast tumors in nude mice with an intravenously injected light-emitting oncolytic vaccinia virus. *Cancer Res.* 2007;67:10038–10046.
- Hales LM, Knowles NJ, Reddy PS, Xu L, Hay C, Hallenbeck PL. Complete genome sequence analysis of Seneca Valley virus-001, a novel oncolytic picornavirus. *J Gen Virol.* 2008;89:1265–1275.
- Reddy PS, Burroughs KD, Hales LM, et al. Seneca Valley virus, a systemically deliverable oncolytic picornavirus, and the treatment of neuroendocrine cancers. *J Natl Cancer Inst.* 2007;99:1623–1633.
- Venkataraman S, Reddy SP, Loo J, Idamakanti N, Hallenbeck PL, Reddy VS. Structure of Seneca Valley virus-001: an oncolytic picornavirus representing a new genus. *Structure.* 2008;16:1555–1561.

31. Venkataraman S, Reddy SP, Loo J, Idamakanti N, Hallenbeck PL, Reddy VS. Crystallization and preliminary X-ray diffraction studies of Seneca Valley virus-001, a new member of the Picornaviridae family. *Acta Crystallogr Sect F Struct Biol Cryst Commun.* 2008;64:293–296.
32. Wadhwa L, Hurwitz MY, Chevez-Barrios P, Hurwitz RL. Treatment of invasive retinoblastoma in a murine model using an oncolytic picornavirus. *Cancer Res.* 2007;67:10653–10656.
33. Sasai K, Romer JT, Lee Y, et al. Shh pathway activity is down-regulated in cultured medulloblastoma cells: implications for preclinical studies. *Cancer Res.* 2006;66:4215–4222.
34. Lee J, Kotliarova S, Kotliarov Y, et al. Tumor stem cells derived from glioblastomas cultured in bFGF and EGF more closely mirror the phenotype and genotype of primary tumors than do serum-cultured cell lines. *Cancer Cell.* 2006;9:391–403.
35. Shu Q, Wong KK, Su JM, et al. Direct orthotopic transplantation of fresh surgical specimen preserves CD133+ tumor cells in clinically relevant mouse models of medulloblastoma and glioma. *Stem Cells.* 2008;26:1414–1424.
36. Li XN, Shu Q, Su JM, Perlaky L, Blaney SM, Lau CC. Valproic acid induces growth arrest, apoptosis, and senescence in medulloblastomas by increasing histone hyperacetylation and regulating expression of p21Cip1, CDK4, and CMYC. *Mol Cancer Ther.* 2005;4:1912–1922.
37. Shu Q, Antalffy B, Su JM, et al. Valproic acid prolongs survival time of severe combined immunodeficient mice bearing intracerebellar orthotopic medulloblastoma xenografts. *Clin Cancer Res.* 2006;12:4687–4694.
38. Read TA, Fogarty MP, Markant SL, et al. Identification of CD15 as a marker for tumor-propagating cells in a mouse model of medulloblastoma. *Cancer Cell.* 2009;15:135–147.
39. Mao XG, Zhang X, Xue XY, et al. Brain tumor stem-like cells identified by neural stem cell marker CD15. *Transl Oncol.* 2009;2:247–257.
40. Panchision DM, Chen HL, Pistollato F, Papini D, Ni HT, Hawley TS. Optimized flow cytometric analysis of central nervous system tissue reveals novel functional relationships among cells expressing CD133, CD15, and CD24. *Stem Cells.* 2007;25:1560–1570.
41. Ward RJ, Lee L, Graham K, et al. Multipotent CD15+ cancer stem cells in patched-1-deficient mouse medulloblastoma. *Cancer Res.* 2009;69:4682–4690.
42. Son MJ, Woolard K, Nam DH, Lee J, Fine HA. SSEA-1 is an enrichment marker for tumor-initiating cells in human glioblastoma. *Cell Stem Cell.* 2009;4:440–452.
43. Huang EH, Hynes MJ, Zhang T, et al. Aldehyde dehydrogenase 1 is a marker for normal and malignant human colonic stem cells (SC) and tracks SC overpopulation during colon tumorigenesis. *Cancer Res.* 2009;69:3382–3389.
44. Labarge MA, Bissell MJ. Is CD133 a marker of metastatic colon cancer stem cells? *J Clin Invest.* 2008;118:2021–2024.
45. Beier D, Hau P, Proescholdt M, et al. CD133(+) and CD133(-) glioblastoma-derived cancer stem cells show differential growth characteristics and molecular profiles. *Cancer Res.* 2007;67:4010–4015.
46. Florek M, Haase M, Marzesco AM, et al. Prominin-1/CD133, a neural and hematopoietic stem cell marker, is expressed in adult human differentiated cells and certain types of kidney cancer. *Cell Tissue Res.* 2005;319:15–26.
47. Jackson WT, Giddings TH, Jr, Taylor MP, et al. Subversion of cellular autophagosomal machinery by RNA viruses. *PLoS Biol.* 2005;3:e156.
48. Kirkegaard K, Taylor MP, Jackson WT. Cellular autophagy: surrender, avoidance and subversion by microorganisms. *Nat Rev Microbiol.* 2004;2:301–314.
49. Klionsky DJ, Abeliovich H, Agostinis P, et al. Guidelines for the use and interpretation of assays for monitoring autophagy in higher eukaryotes. *Autophagy.* 2008;4:151–175.
50. Wong J, Zhang J, Si X, et al. Autophagosome supports coxsackievirus B3 replication in host cells. *J Virol.* 2008;82:9143–9153.
51. Jackson WT, Giddings TH, Jr, Taylor MP, et al. Subversion of cellular autophagosomal machinery by RNA viruses. *PLoS Biol.* 2005;3:e156.
52. Sun Y, Kong W, Falk A, et al. CD133 (Prominin) negative human neural stem cells are clonogenic and tripotent. *PLoS One.* 2009;4:e5498.
53. Wang J, Sakariassen PO, Tsinkalovsky O, et al. CD133 negative glioma cells form tumors in nude rats and give rise to CD133 positive cells. *Int J Cancer.* 2008;122:761–768.
54. Chaichana K, Zamora-Berridi G, Camara-Quintana J, Quinones-Hinojosa A. Neurosphere assays: growth factors and hormone differences in tumor and nontumor studies. *Stem Cells.* 2006;24:2851–2857.
55. Cordey M, Limacher M, Kobel S, Taylor V, Lutolf MP. Enhancing the reliability and throughput of neurosphere culture on hydrogel microwell arrays. *Stem Cells.* 2008;26:2586–2594.
56. Mathew R, Karantza-Wadsworth V, White E. Role of autophagy in cancer. *Nat Rev Cancer.* 2007;7:961–967.
57. Liu Y, Schiff M, Czymmek K, Talloczy Z, Levine B, Nesh-Kumar SP. Autophagy regulates programmed cell death during the plant innate immune response. *Cell.* 2005;121:567–577.
58. Mizushima N. Autophagy: process and function. *Genes Dev.* 2007;21:2861–2873.
59. Brabec-Zaruba M, Berka U, Blaas D, Fuchs R. Induction of autophagy does not affect human rhinovirus type 2 production. *J Virol.* 2007;81:10815–10817.
60. Zhou Z, Jiang X, Liu D, et al. Autophagy is involved in influenza A virus replication. *Autophagy.* 2009;5:321–328.
61. Taylor MP, Jackson WT. Viruses and arrested autophagosome development. *Autophagy.* 2009;5:870–871.
62. Liu TC, Kim D. Gene therapy progress and prospects cancer: oncolytic viruses. *Gene Ther.* 2008;15:877–884.
63. Hicks AM, Riedinger G, Willingham MC, et al. Transferable anticancer innate immunity in spontaneous regression/complete resistance mice. *Proc Natl Acad Sci USA.* 2006;103:7753–7758.